Vortex Sheet in Rotating Superfluid ^{3}He-A

Ü. Parts, E.V. Thuneberg, G.E. Volovik,* J.H. Koivuniemi, V.M.H. Ruutu, M. Heinilä, J.M. Karimäki, and M. Krusius
Low Temperature Laboratory, Helsinki University of Technology, 02150 Espoo, Finland
(Received 7 April 1994)

A new state of rotating superfluid ^{3}He-A has been found. Instead of quantized vortex lines, it consists of a continuous vortex sheet. The sheet has as a backbone a topologically stable domain wall called soliton, to which the vorticity is bound. The sheet folds to equidistant layers that fill uniformly the rotating container. The new state can easily be created experimentally in spite of its higher energy. Its identification is deduced from nuclear magnetic resonance.

PACS numbers: 67.57.Fg, 47.32.Cc, 74.20.De

Symmetry-breaking phase transitions lead to ordered systems in which topologically stable defects can exist. A recurring configuration is the confinement of one object to another of higher dimensionality. Such topological confinement can be divided into two types: (i) An object may serve as a boundary for a higher dimensional object, or (ii) an object may exist only within another object, from which it cannot escape to the world outside. Examples of the former type are a monopole as a termination point of a disclination line in liquid crystals [1], a cosmic domain wall with a string as its edge line [2], an antiphase boundary terminating to a dislocation line in ordered binary alloys [3], the planar soliton in superfluid ^{3}He-B emanating from a vortex line [4], and a possible half-quantum vortex confined to the borderline of three crystal grains in unconventional superconductors [5]. A well-known example of the latter type is a Bloch line within a domain wall in ferromagnets [3].

Here we report an observation of the latter kind of confinement in rotating ^{3}He-A. The higher dimensional object is a topologically stable domain wall, called soliton. The corresponding one-dimensional object turns out to be a specific type of quantized vortex line, which exists only within the soliton. A soliton with an array of such vortices forms a vortex sheet that we call a *vortex soliton.* This object is supported by rotation. It uniformly fills the rotating container by folding into equidistant layers, as illustrated in Fig. 1.

Historically, vorticity concentrated in sheets was suggested by Onsager [6] and London [7] to describe the superfluid state of ^{4}He under rotation. It turned out, however, that a vortex sheet is unstable towards breakup into separate quantized vortex lines in ^{4}He. Nevertheless, a later calculation of the spacing between vortex sheets by Landau and Lifshitz [8], who did not impose a quantization requirement on the sheets, happens to be exactly to the point for the vortex soliton in ^{3}He-A.

Small-scale structure.—The anisotropy of ^{3}He-A is described by two unit vectors: $\hat{\mathbf{d}}$ is the spin quantization axis and $\hat{\mathbf{l}}$ is the orbital angular momentum axis [9]. These are coupled only weakly by the dipole-dipole interaction energy $f_D = -\frac{1}{2}g_D(\hat{\mathbf{d}}\cdot\hat{\mathbf{l}})^2$. It follows that the ground state of the liquid is dipole locked, $\hat{\mathbf{d}} = \pm\hat{\mathbf{l}}$. The soliton is a surface separating domains having parallel and antiparallel orientations of $\hat{\mathbf{d}}$ and $\hat{\mathbf{l}}$. The core of the soliton has a smooth bending of $\hat{\mathbf{d}}$ and $\hat{\mathbf{l}}$ [10]. A large energy barrier prevents the breakup of this surface into separate pieces because a cut would require the nucleation of singularities in the $\hat{\mathbf{d}}$ field [11]. Solitons are often created in inhomogeneous transitions into the superfluid state, and are well known from NMR measurements [12]. In the following we will assume a magnetic field $H \gg 3\,\mathrm{mT}$, which fixes $\hat{\mathbf{d}}$ perpendicular to $\mathbf{H}$.

The soliton has two degenerate states, which can be obtained from each other by a symmetry operation. The degeneracy gives rise to a topological object, a kink, separating two states; see Fig. 2(a). The kink has no singularity in the $\hat{\mathbf{d}}$ and $\hat{\mathbf{l}}$ fields and is equivalent to the Bloch line. The topological characteristic of such lines is $\nu_l = (1/4\pi)\int dx\,dy\,\hat{\mathbf{l}}\cdot(\partial_x\hat{\mathbf{l}}\times\partial_y\hat{\mathbf{l}})$. This is the normalized area which $\hat{\mathbf{l}}(\mathbf{r})$ sweeps on a unit sphere while $\mathbf{r}$ varies on the cross-sectional plane of the line. For one kink this invariant is fractional $\nu_l = \pm 1/2$. Because of the magnetic field, the corresponding invariant for $\hat{\mathbf{d}}$ is trivial, $\nu_d = 0$.

The specific property of ^{3}He-A is that the circulation of the superfluid velocity is directly related to the $\hat{\mathbf{l}}$ texture [13]: The circulation on a closed path around a kink is $\oint \mathbf{v}_s\cdot d\mathbf{r} = 2\kappa\nu_l$, where $\kappa = h/2m$ is the circulation quan-

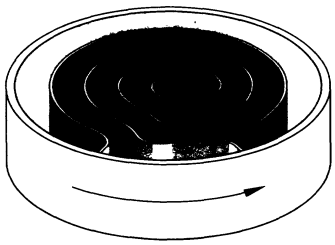

FIG. 1. Macroscopic structure of the vortex soliton in our cylindrical container rotating at $\Omega = 0.58$ rad/s. The structure is calculated assuming one sheet in contact with the wall, and following a local minimum of energy during increasing Ω. The energy is approximated by the leading terms (isotropic kinetic energy and surface energy).

0031-9007/94/72(24)/3839(4)$06.00

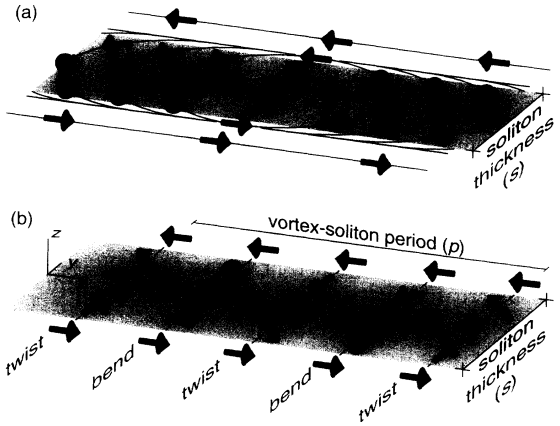

FIG. 2. Schematic small-scale structure of (a) a kink in a soliton and (b) a vortex soliton. The soliton wall is along the x-z plane, the vortices are parallel to the z axis, and $\mathbf{H} \perp \hat{\mathbf{x}}$. The arrows denote the unit vector $\hat{\mathbf{l}}$ whereas $\hat{\mathbf{d}} \approx \hat{\mathbf{x}}$. In the vortex soliton (b), the kinks form a periodic structure with alternating twist and bend sections.

tum. This means that the kink represents a nonsingular vortex with the quantum number $N = 2\nu_l = \pm 1$.

The kinks can be used as building blocks for larger objects. Two cases are of interest here. The first object is constructed by closing a soliton sheet to cylindrical shape. A cylinder without kinks would probably shrink away. The minimum number of kinks is two because $\nu_l - \nu_d$ has to be integer for an object surrounded by dipole-locked liquid. When the kinks have the same sign of circulation, i.e., the total $N = \pm 2$, the cylinder cannot disappear. This minimal soliton cylinder is nothing but the (two-quantum) vortex usually observed in NMR experiments [14]. The opposite limiting case is the vortex soliton with very large N. There the kinks form a periodic structure; see Fig. 2(b). The structure alternates between a twist and a bend of $\hat{\mathbf{l}}$ in intervals of $p/4$. The period p, containing two quanta of circulation, is determined by the usual condition that the density of circulation quanta equals $2\Omega/\kappa$, where Ω is the angular velocity of rotation. Thus $p = \kappa/\Omega b$ where b is the distance between the sheets.

The vortex soliton is energetically stable against dissociation into two-quantum vortices. This is because the distance between quanta in the vortex soliton ($p/2$; see below) is larger than in the two-quantum vortex ($\approx 30\,\mu$m), and energy is required to push the quanta closer to each other.

Macroscopic structure.—Let us find b, the equilibrium distance between the sheets, in a container rotating with $\mathbf{\Omega} \parallel \mathbf{H} \parallel \hat{\mathbf{z}}$. It is determined by the competition of the surface tension σ of the vortex soliton and the kinetic energy of the counterflow $\mathbf{v} = \mathbf{v}_n - \mathbf{v}_s$ outside the sheet. Locally the folded sheet can be considered as a system of planes. The motion of the normal component, which corresponds to the vorticity $\nabla \times \mathbf{v}_n = 2\Omega\hat{\mathbf{z}}$, can be represented by the shear flow $\mathbf{v}_n = -2\Omega y\hat{\mathbf{x}}$ parallel to the planes. In the gap between nearest planes, the vortex-free $\mathbf{v}_s$ is constant and equals the average $\mathbf{v}_n$ to minimize the counterflow. Thus the velocity jump across the vortex sheet is $\Delta\mathbf{v}_s = 2\Omega b\hat{\mathbf{x}}$. The counterflow energy per volume is $(1/b)\int \frac{1}{2}\rho_{s\parallel}v^2\,dy = \frac{1}{6}\rho_{s\parallel}\Omega^2 b^2$, where $\rho_{s\parallel}$ is the superfluid density for the flow along $\hat{\mathbf{l}}$. The surface energy per volume equals σ/b. Minimizing their sum with respect to b one obtains the anisotropic version of the result in Ref. [8],

$$b = \left(\frac{3\sigma}{\rho_{s\parallel}\Omega^2}\right)^{1/3}. \qquad (1)$$

Substituting $\rho_{s\parallel}$ and σ (see below), Eq. (1) yields $b = 360\,\mu$m at $\Omega = 1$ rad/s, which is comparable to the nearest-neighbor distance of 280 μm in an array of two-quantum vortices. This macroscopic description of the rotational state of Fig. 1 becomes inadequate only at small $\Omega \approx 0.05$ rad/s, where b becomes comparable to the size of our container.

Experiment.—NMR measurements were performed on a cylindrical container with radius $R = 2.5$ mm and height 7 mm. Both the rotation $\mathbf{\Omega}$ and the magnetic field $\mathbf{H}$ are axial. The transverse NMR absorption spectrum is shown in Fig. 3. The various resonance frequencies are customarily expressed as $\omega^2 = \omega_0^2 + R_\perp^2\omega_\parallel^2$. Here $\omega_0 = \gamma H$ is the Larmor frequency and $\omega_\parallel$ the longitudinal resonance frequency of the A phase. The main absorption peak at $R_\perp = 1$ arises from dipole-locked regions. The temperature dependence of $\omega_\parallel$ was used for thermometry. The frequency shifted satellite peaks with $R_\perp < 1$ result from the excitation of spin-wave modes localized in the dipole-unlocked ($\hat{\mathbf{d}} \neq \pm\hat{\mathbf{l}}$) regions. The peaks marked with $R_\perp = 0.86$ and $R_\perp = 0.81$ in Fig. 3 represent solitons, which often appear after rapid cooling into the superfluid state. These satellites disappear under rotation while new ones appear signifying the presence of vorticity. The satellite at $R_\perp = 0.64$ corresponds to the equilibrium array of two-quantum vortices [14]. The larger peak at $R_\perp = 0.66$ has been observed in earlier experiments but its origin remained unexplained [14]. We find that it is shifted in frequency relative to the usual vortex satellite. We associate it with the vortex soliton. This conclusion can be reached in several different ways, some of which will be discussed below.

Creation.—The creation of the vortex-soliton state under slow acceleration depends on the initial state before the rotation is started. If there are no solitons in the vessel, the acceleration results in the ordinary vortex signal $R_\perp = 0.64$ of Fig. 3. The same result is obtained by starting from the state marked with $R_\perp = 0.86$. There the satellite peak is associated with a soliton perpendicular to the field $\mathbf{H}$ [10]. However, if the rotation is started in the state $R_\perp = 0.81$, even with an acceleration as small as $d\Omega/dt \approx 10^{-4}$ rad/s^2, the vortex-soliton signal ($R_\perp = 0.66$) results. The satellite at $R_\perp = 0.81$ comes

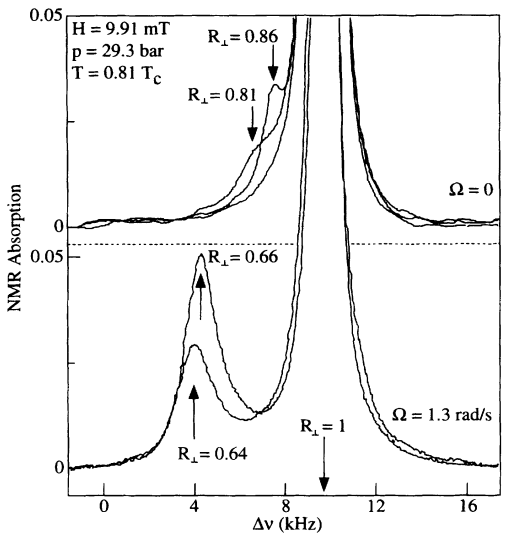

FIG. 3. The cw NMR absorption spectrum. The frequency shift $\Delta\nu = \nu - \nu_0$ is measured from the Larmor frequency ν_0. All spectra have their main peak roughly at $R_\perp = 1$. Satellite absorption peaks with varying frequency shifts are formed by topological objects. The two lower spectra are measured under rotation. The peak at $R_\perp = 0.64$ arises from the usual vortex state, which consists of two-quantum vortex lines, and $R_\perp = 0.66$ we associate with the vortex-soliton state. The three upper spectra are recorded at $\Omega = 0$ right after cooldown into the superfluid state. One of them shows no satellite peak; the vertical scale of the figure is normalized to the height of its $R_\perp = 1$ peak. The two additional spectra display satellite peaks which arise from solitons. When rotated, the state marked with $R_\perp = 0.81$ (soliton with plane $\parallel \boldsymbol{\Omega}$) gives rise to the vortex soliton, whereas the two other states (soliton peak absent or at $R_\perp = 0.86$) result in vortex lines.

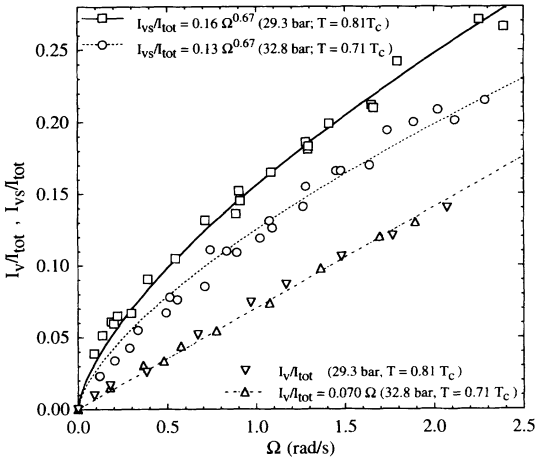

FIG. 4. Integrated NMR absorption of the satellite peaks at $R_\perp \sim 0.6$ as a function of the rotation velocity Ω. The fitted curves agree with theory for both the vortex ($I_v \propto \Omega$) and the vortex-soliton ($I_{vs} \propto \Omega^{2/3}$) states. The data are normalized to the total NMR absorption $I_{\rm tot}$.

from a soliton with its plane approximately parallel to $\mathbf{H} \parallel \boldsymbol{\Omega}$. This was the first clue that the large satellite ($R_\perp = 0.66$) originates from vorticity accumulated within a soliton $\parallel \boldsymbol{\Omega}$.

Only two out of twenty rapid cooldowns produced the soliton state $R_\perp = 0.81$, which gave rise to the vortex-soliton state. A practical way to create the vortex soliton is periodic modulation of Ω. The drive can be sinusoidal $\Omega = \Delta\Omega \sin(2\pi t/\tau)$ with an amplitude $\Delta\Omega \geq 0.3$ rad/s and a period $\tau \leq 30$ s. The vortex-soliton state is invariably found to evolve from any initial state if the modulation remains switched on for several minutes. Sometimes it could also be created by one sharp acceleration.

Once created, it was possible to grow and shrink the vortex soliton by changing Ω. The state showed no decay at temperatures below $0.9T_c$, and only slow decay at higher temperatures. In fact, it was difficult to get rid of the vortex soliton: Even 1 h after stopping the cryostat, it was sometimes recovered by slow acceleration.

NMR absorption.—Some properties of the vortex soliton can be calculated analytically in the limit that the thickness of the soliton s is much smaller than the period p (Fig. 2). This is a reasonable approximation since theoretically $s \approx 12\,\mu$m and $p = 180\,\mu$m at $\Omega = 1$ rad/s. We find that both the surface tension σ in Eq. (1) and the NMR frequency are determined by the twist section, which has the lowest energy. The condition $s \ll p$ allows us to neglect the derivatives along the soliton, and we get following the procedure of Ref. [10] that $\sigma = 2\sqrt{K_t g_D}$ and

$$R_\perp^2 = \frac{K_6}{2K_t}\left(\sqrt{1+\frac{8K_t}{K_6}} - 1\right) - 1\,. \qquad (2)$$

Here K_t and K_6 are bending-energy coefficients defined and tabulated in Ref. [15]. The calculated frequency agrees with the observed one. The usual two-quantum vortex and the vortex soliton are exceptional because of their low values of $R_\perp$. All other extended objects in bulk liquid (singular vortices, vortex-free solitons) have higher values, and thus cannot explain the experimental observations.

The intensity of the satellite peaks as a function of the rotation velocity is plotted in Fig. 4. The vortex peak grows linearly with Ω. This is natural because each vortex contributes individually to the absorption, and their number is linear in Ω. The vortex-soliton peak behaves distinctly differently, being approximately proportional to $\Omega^{2/3}$. This dependence cannot be explained by a different structure of separated vortex lines. Instead, the vortex sheet offers a simple explanation: The absorption is expected to be proportional to the length of the soliton (in the plane $\perp \boldsymbol{\Omega}$), which equals $\pi R^2/b \propto \Omega^{2/3}$. Our calculation also gives the prefactor to the $\Omega^{2/3}$ dependence in agreement with experiment.

Growth.—A state with a given amount of circulation can be stable only at rotation velocities in some interval

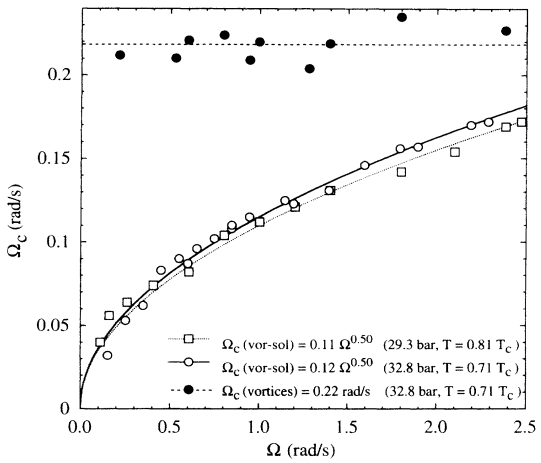

FIG. 5. Critical angular velocity Ω_c for nucleating new vorticity in the absence (filled circles) and in the presence of the vortex soliton (open circles and squares). In the latter case the new vorticity will appear in the vortex soliton, whereas in the former case it appears as separate vortex lines.

$\Omega_1 < \Omega < \Omega_2$. For $\Omega < \Omega_1$ vorticity will annihilate on the side wall of the container, while at $\Omega > \Omega_2$ new vorticity is created. The width of this window is defined as the critical angular velocity $\Omega_c = \Omega_2 - \Omega_1$. Figure 5 shows that the measured Ω_c depends on whether the vortex soliton is present or not. In its absence, usual vortices are created, and Ω_c is constant. This can be understood so that a new vortex will nucleate whenever a critical value v_c of the counterflow velocity $\mathbf{v} = \mathbf{v}_n - \mathbf{v}_s$ is reached at the wall of the container. Because here $v = (\Omega - \Omega_1)R$, it follows that $\Omega_c = v_c/R$ is constant ≈ 0.2 rad/s in our experimental setup.

The presence of the vortex soliton leads to a reduced Ω_c. The sheet grows when Ω exceeds Ω_2; i.e., the new vorticity is added to it and not as separate vortex lines. From the low Ω_c we deduce that the vortex soliton has to be in contact with the cylindrical wall of the container. This is because a closed sheet cannot change its circulation (except by emitting or absorbing vortices). In contrast, new vorticity can relatively easily enter the sheet at the line of contact with the cylindrical cell wall. The lower Ω_c in the vortex-soliton state explains why this state can be grown in spite of its presumably larger energy compared to the usual vortex state.

The Ω_c of the vortex soliton can be qualitatively understood by postulating that the length scale determining v_c is the core size of the vortex kink. This gives $\Omega_c R \approx \kappa/p \approx \Omega b \propto \Omega^{1/3}$, which roughly explains both the order of magnitude and the dependence on Ω.

The vortex soliton cannot be created in zero field but if created in higher field, it remains metastable also at $H = 0$ showing only slow decay. This can be qualitatively understood so that the vortex soliton remains essentially unchanged at $H = 0$, but Ω_c for vortex lines is only one-half of the value at high field.

In conclusion, the vortex soliton can easily be generated experimentally in rotating ^{3}He-A. Its stability arises from the special combination of one- and two-dimensional topological objects. Its macroscopic form consists of contact lines with the container wall and folding to equidistant layers whose density increases with increasing rotation velocity. It represents a new way of superfluids to respond to rotation. A similar state could exist in unconventional superconductors for which some models incorporate the necessary ingredients of broken time-inversion symmetry and order-parameter domain walls.

* Permanent address: Landau Institute for Theoretical Physics, 117334 Moscow, Russia.

[1] M. Kléman, Rep. Prog. Phys. **52**, 555 (1989); I. Chuang, N. Turok, and B. Yurke, Phys. Rev. Lett. **66**, 2472 (1991).

[2] A. Vilenkin and E.P.S. Shellard, *Cosmic Strings and Other Topological Defects* (Cambridge Univ. Press, Cambridge, 1993).

[3] Chih-Wen Chen, *Magnetism and Metallurgy of Soft Magnetic Materials* (North-Holland, Amsterdam, 1977).

[4] Y. Kondo, J. Korhonen, M. Krusius, V. Dmitriev, E. Thuneberg, and G. Volovik, Phys. Rev. Lett. **68**, 3331 (1992); Phys. Rev. B **47**, 8868 (1993).

[5] V. Geshkenbein, A. Larkin, and A. Barone, Phys. Rev. B **36**, 235 (1987).

[6] L. Onsager (unpublished); see F. London, *Superfluids* (Wiley, New York, 1990), Vol. II, p 151.

[7] H. London, in *Report of International Conference on Fundamental Particles and Low Temperatures* (Physical Society, London, 1946), Vol. II, p. 48.

[8] L. Landau and E. Lifshitz, Dokl. Akad. Nauk. **100**, 669 (1955).

[9] D. Vollhardt and P. Wölfle, *The Superfluid Phases of Helium 3* (Taylor & Francis, London, 1990).

[10] K. Maki and P. Kumar, Phys. Rev. B **17**, 1088 (1978).

[11] Cutting the soliton is not excluded because the sign of $\hat{\mathbf{d}}$ is not generally defined, and thus half-quantum vortices become possible; see G. Volovik, *Exotic Properties of Superfluid ^{3}He* (World Scientific, Singapore, 1992); M. Salomaa and G. Volovik, Rev. Mod. Phys. **59**, 533 (1987). In the absence of singularities, $\hat{\mathbf{d}}$ is uniquely defined everywhere once its sign is fixed at one point.

[12] C. Gould and D. Lee, Phys. Rev. Lett. **37**, 1223 (1976).

[13] N.D. Mermin and T.-L. Ho, Phys. Rev. Lett. **36**, 594 (1976); T.-L. Ho, Phys. Rev. B **18**, 1144 (1978).

[14] P. Hakonen, M. Krusius, and H. Seppälä, J. Low Temp. Phys. **60**, 187 (1985); P. Hakonen, Physica (Amsterdam) **178B**, 83 (1992).

[15] A. Fetter, J. Sauls, and D. Stein, Phys. Rev. B **28**, 5061 (1983).

FIG. 1. Macroscopic structure of the vortex soliton in our cylindrical container rotating at $\Omega = 0.58$ rad/s. The structure is calculated assuming one sheet in contact with the wall, and following a local minimum of energy during increasing Ω. The energy is approximated by the leading terms (isotropic kinetic energy and surface energy).

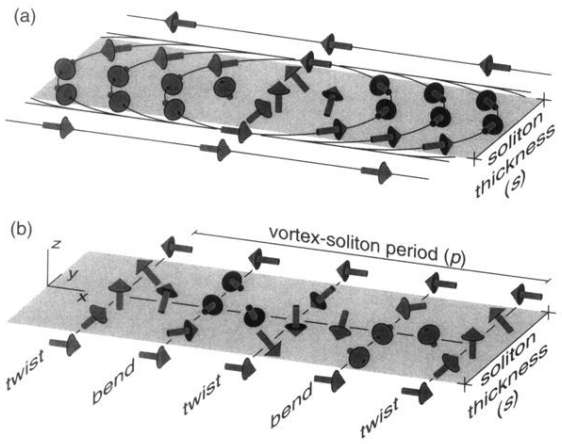

FIG. 2. Schematic small-scale structure of (a) a kink in a soliton and (b) a vortex soliton. The soliton wall is along the x-z plane, the vortices are parallel to the z axis, and $\mathbf{H} \perp \hat{\mathbf{x}}$. The arrows denote the unit vector $\hat{\mathbf{l}}$ whereas $\hat{\mathbf{d}} \approx \hat{\mathbf{x}}$. In the vortex soliton (b), the kinks form a periodic structure with alternating twist and bend sections.